

# Kinetic Energy Conversion in A Wind-forced Submesoscale Flow

Song Li<sup>1,2</sup>, Nuno Serra<sup>1</sup>, Detlef Stammer<sup>1</sup>

<sup>1</sup> Institut für Meereskunde , Center for Earth System Research and Sustainability, Universität Hamburg, Germany; <sup>2</sup>College of Meteorology and Oceanography, National University of Defense Technology, China

## What We Did?

Despite recent progress in measuring the ocean eddy field with satellite missions at the mesoscale (order of 100 km), containing the major fraction of ocean kinetic energy, many questions still remain regarding the generation, conversion and dissipation mechanisms of eddy kinetic energy ( $K_e$ ). In this work, we use the output from an idealized 500-m resolution ocean numerical simulation to study the conversion of  $K_e$  in the absence and presence of wind stress forcing.

## What We For?

- To understand and quantify the main processes behind the forcing of kinetic energy conversion in a surface-intensified submesoscale flow.

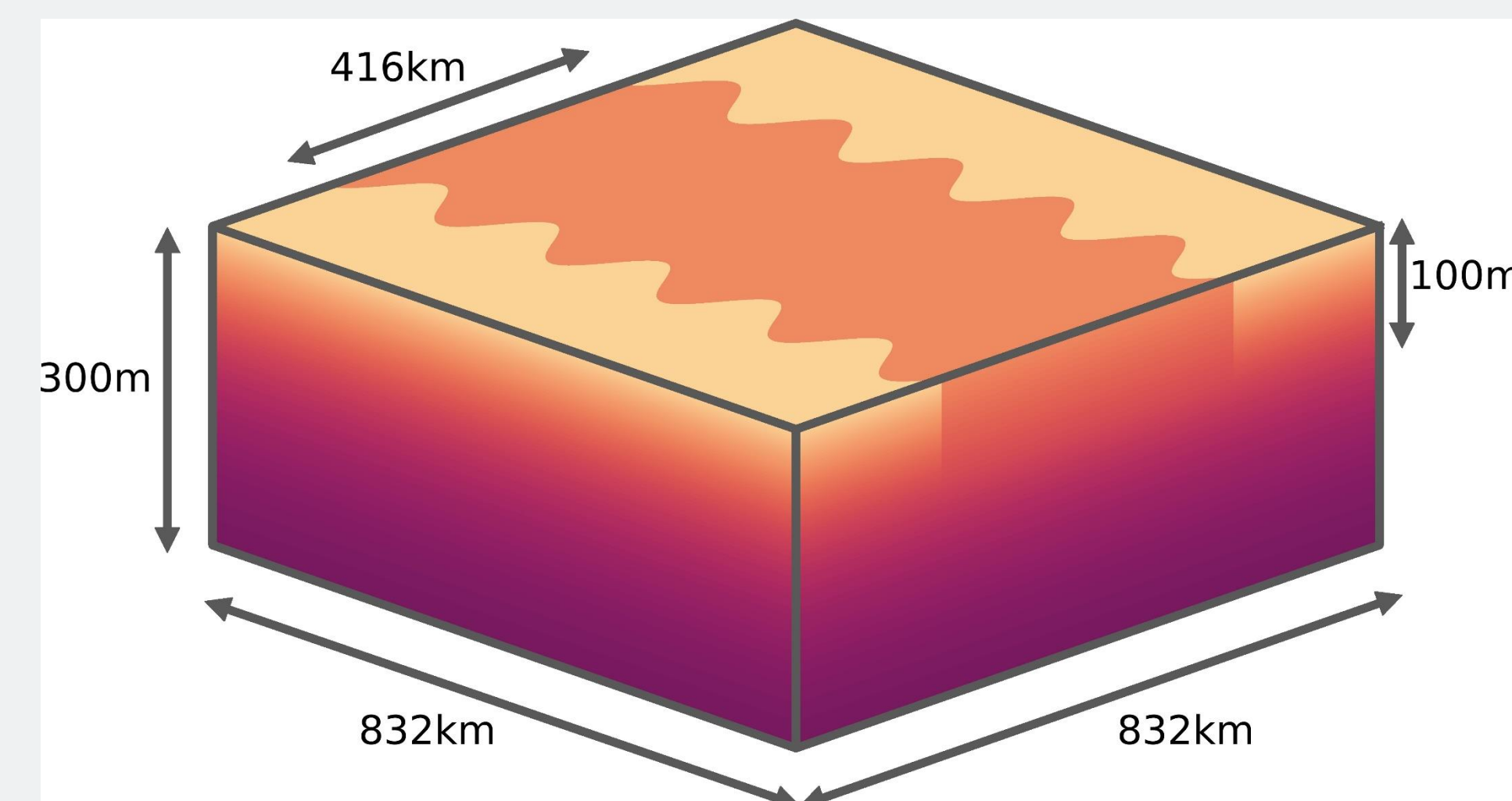


Figure 1 Density distribution of the initial condition..

## Model Configuration

### Domain Setting

- MITgcm with a non-hydrostatic Boussinesq approximation
- f-plane assumption
- 1664x1664x60 idealized box with the resolution of 500m (horizontal) and 5m (vertical)

### Initial Condition

- cold water in the center over the top 100m

### Developing

- First, the box is spinning up until a full eddy field established
- Then, add wind stress every month (wind stress forcing lasts 17 h)

### Analyzing

- Compare the wind case and no wind case

## Description of the Flow Field

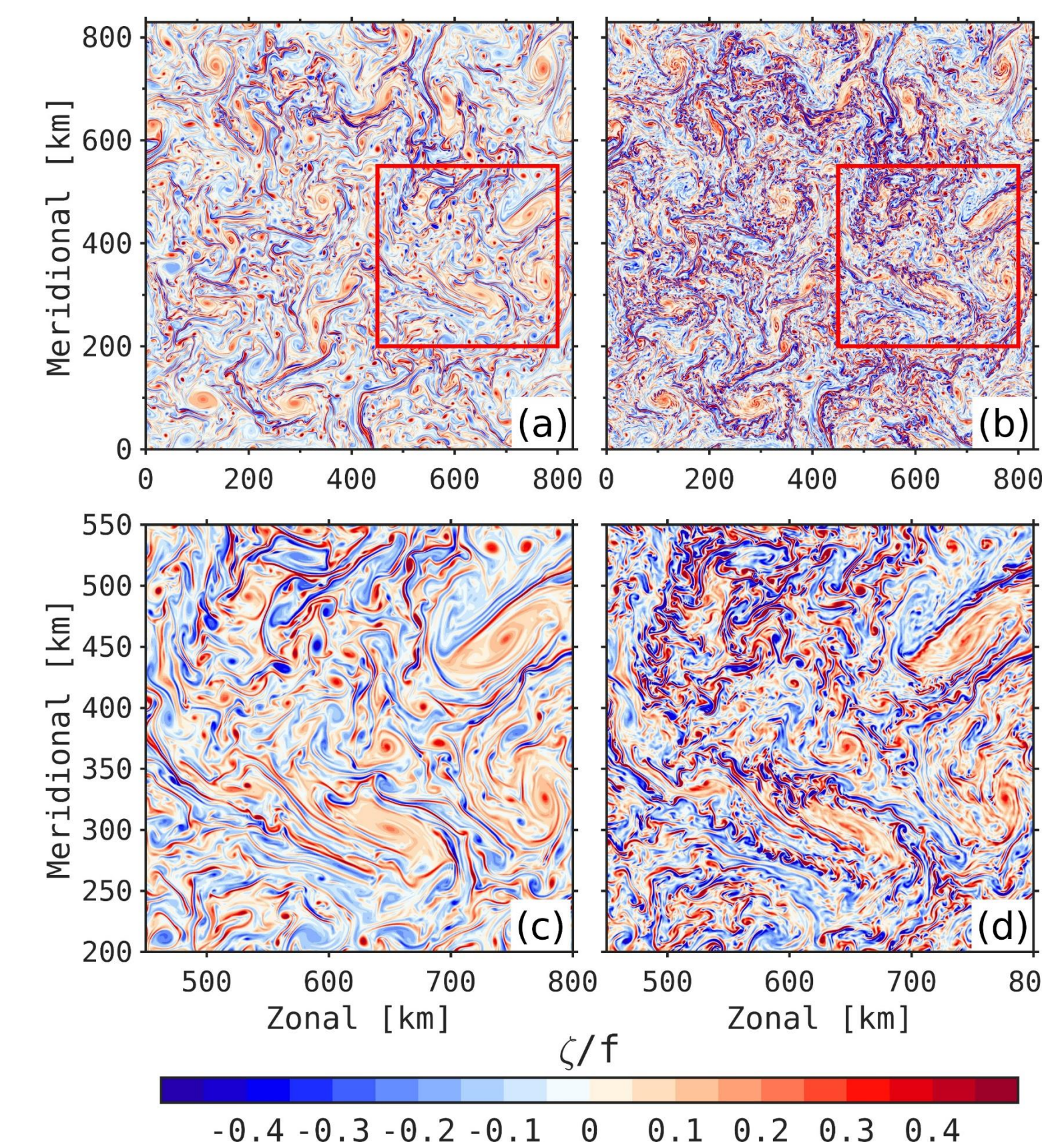


Figure 2 Snapshots of normalized relative vertical vorticity at the surface. (a) No forcing run; (b) wind-forced run. (c) and (d) are zoomed-in domains denoted by the red rectangles in (a) and (b), respectively.

- A significant enhancement of submesoscale motions by wind events.
- Wind events created small steep fronts and introduced strong instability

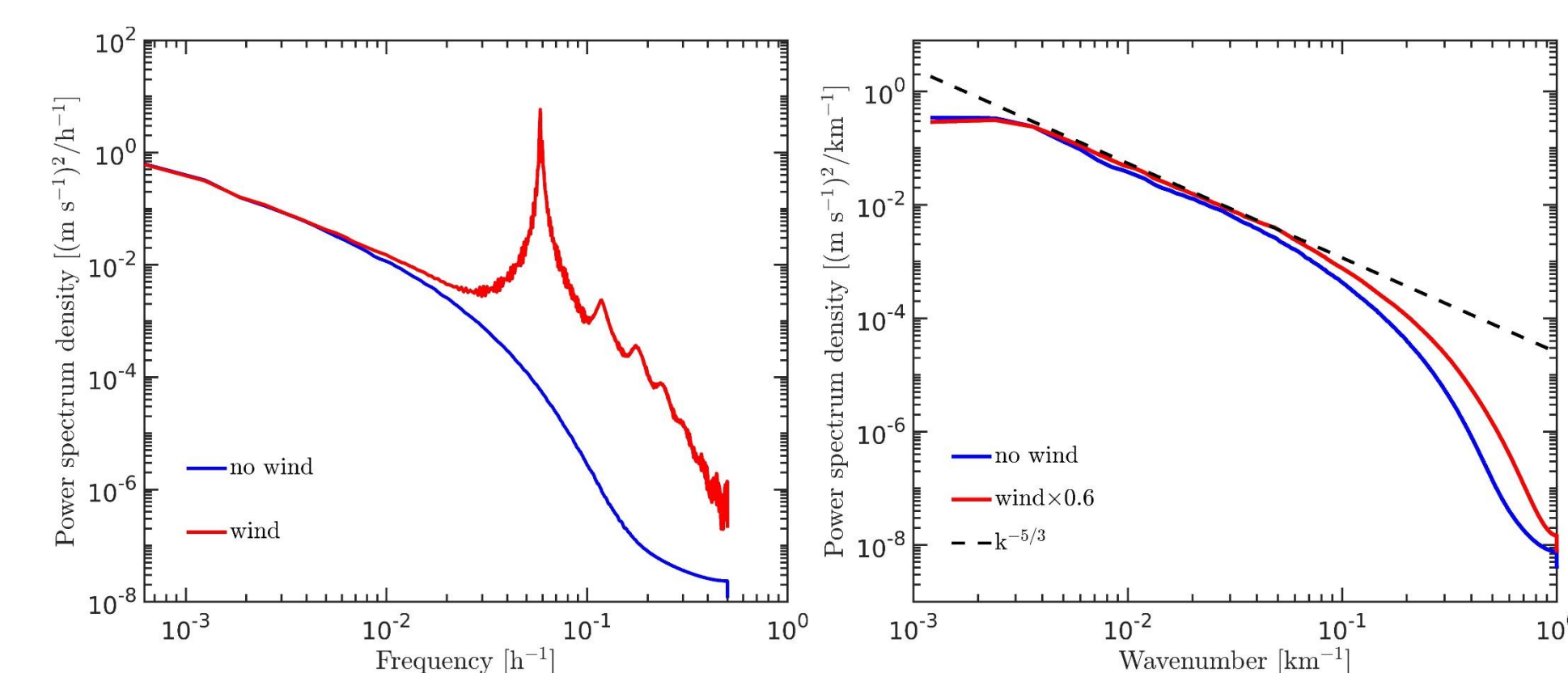


Figure 3 (left) Frequency and (right) wavenumber spectrum of zonal velocity at the surface.

- Variable winds dramatically excited inertial oscillations in the upper ocean
- Currents among all scales were more active in the forced run

## Conversion Between Energy reservoirs

$$C(P_e, P_m) = - \int_V \frac{g}{n_0} \overline{\rho' \mathbf{u}_h'} \cdot \nabla_h \bar{\rho} dV,$$

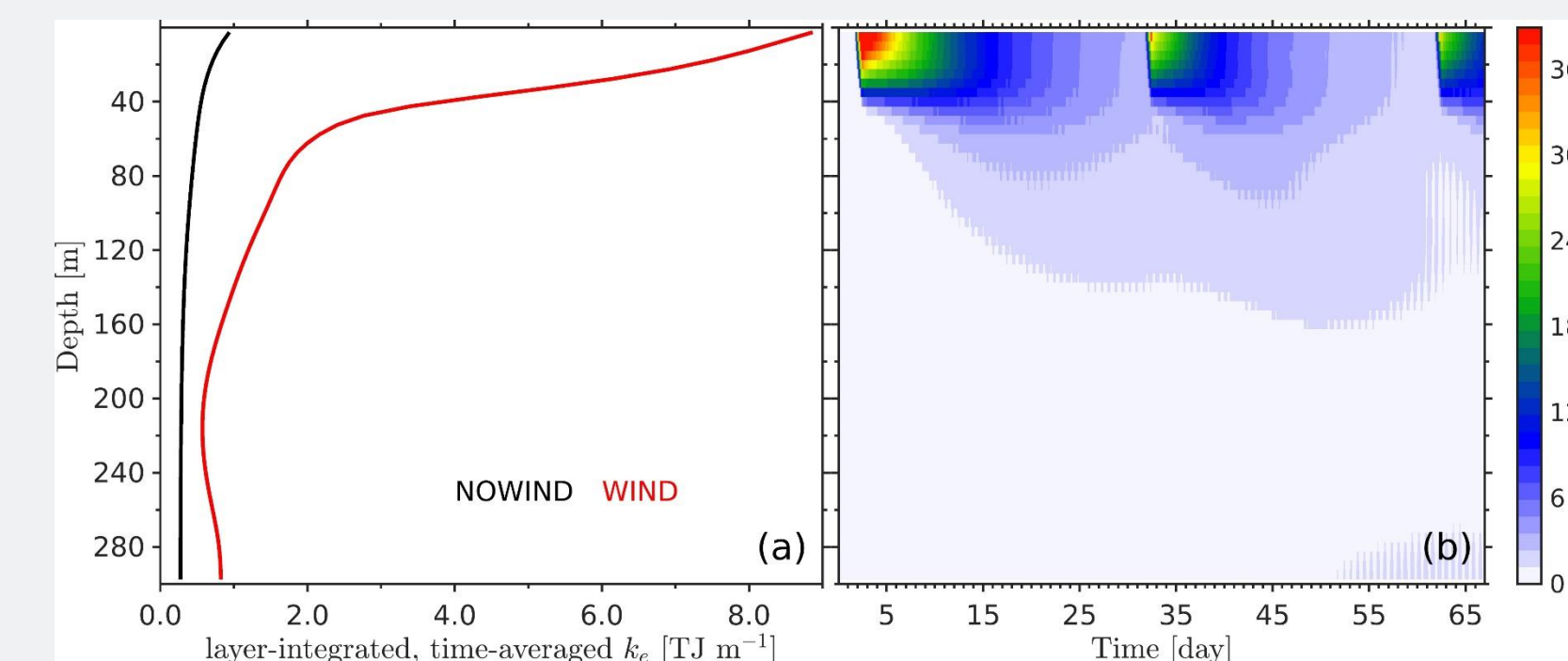


Figure 4 (a) Layer-integrated, time-averaged  $k_e$  profile for the unforced run (black line) and forced run (red line). (b) Variation of layer-mean  $\Delta k_e$  with time and depth.

- $K_e$  increased approximately nine times in the mixed layer and considerably in the pycnocline in the forced run.

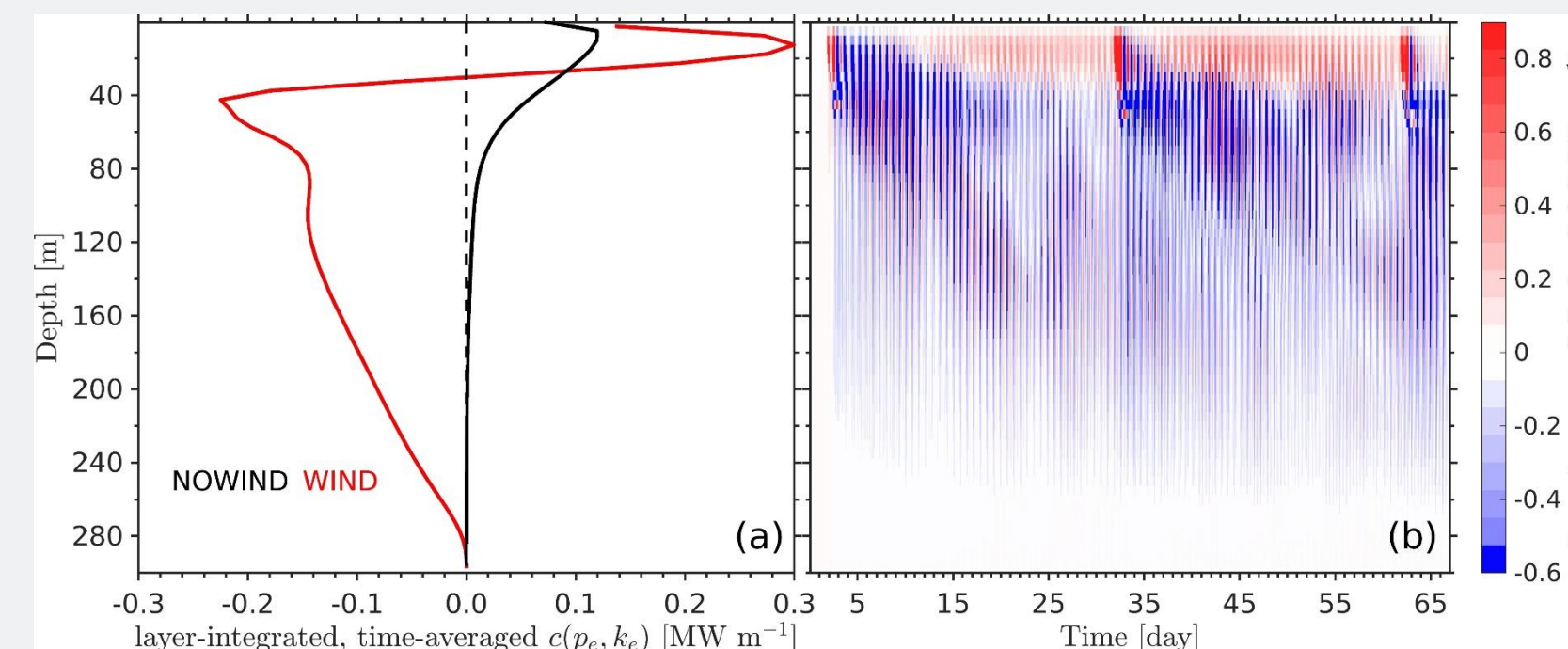


Figure 5 (a) Layer-integrated, time-averaged  $c(p_e, k_e)$  profile for the unforced run (black line) and forced run (red line). (b) Variation of layer-mean  $\Delta c(p_e, k_e)$  with time and depth.

$c(p_e, k_e) > 0$	$p_e \rightarrow k_e$	$\rho' > 0$ and $w' < 0$	downwelling of dense water	flattening of isopycnal
		$\rho' < 0$ and $w' > 0$	upwelling of light water	lowering of isopycnal
$c(p_e, k_e) < 0$	$k_e \rightarrow p_e$	$\rho' > 0$ and $w' > 0$	upwelling of dense water	sloping of isopycnal
		$\rho' < 0$ and $w' < 0$	downwelling of light water	rising of isopycnal

Table 1: All possibilities regarding different signs of  $c(p_e, k_e)$ .

- Baroclinicity reigned in the layers above depth 150 m

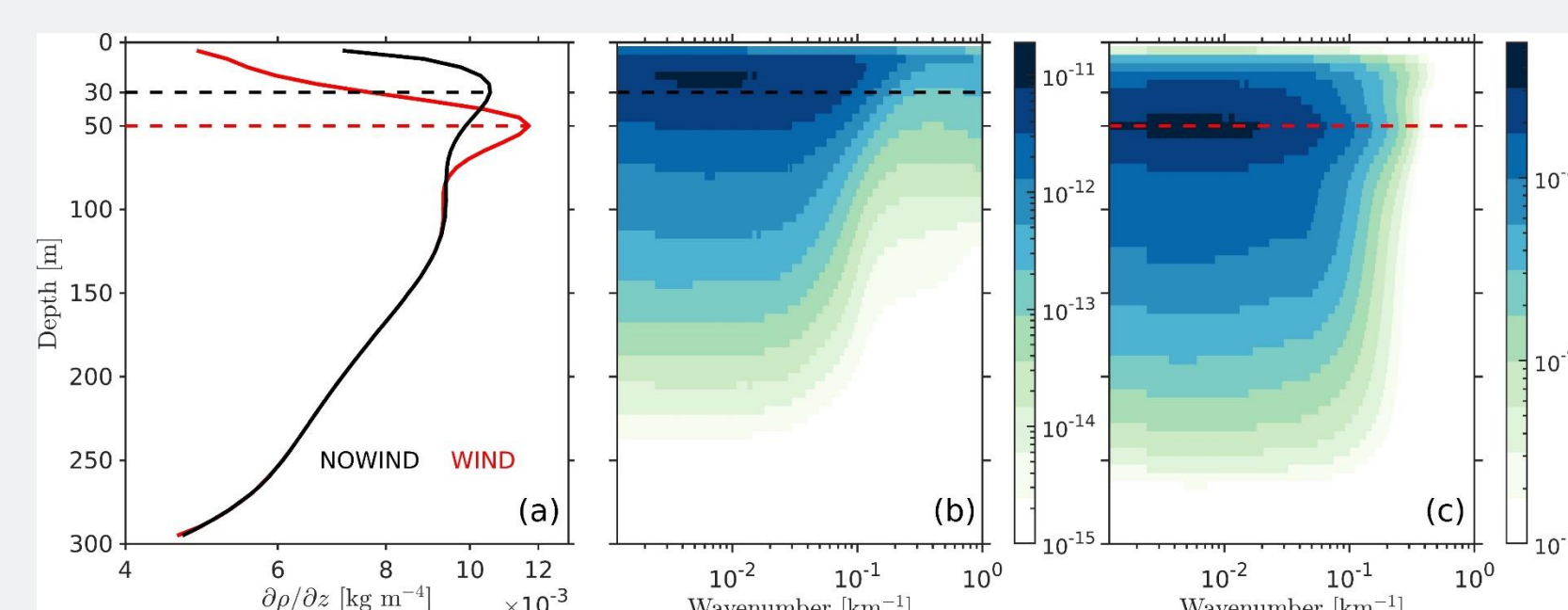


Figure 6 (a) Vertical potential density gradient profile. (b) The wavenumber spectrum of  $c(p_e, k_e)$  for the unforced run and (c) the same as (b) but for the forced run.

- The mixed layer was deepened by wind events.

## Inertial and Superinertial Motions

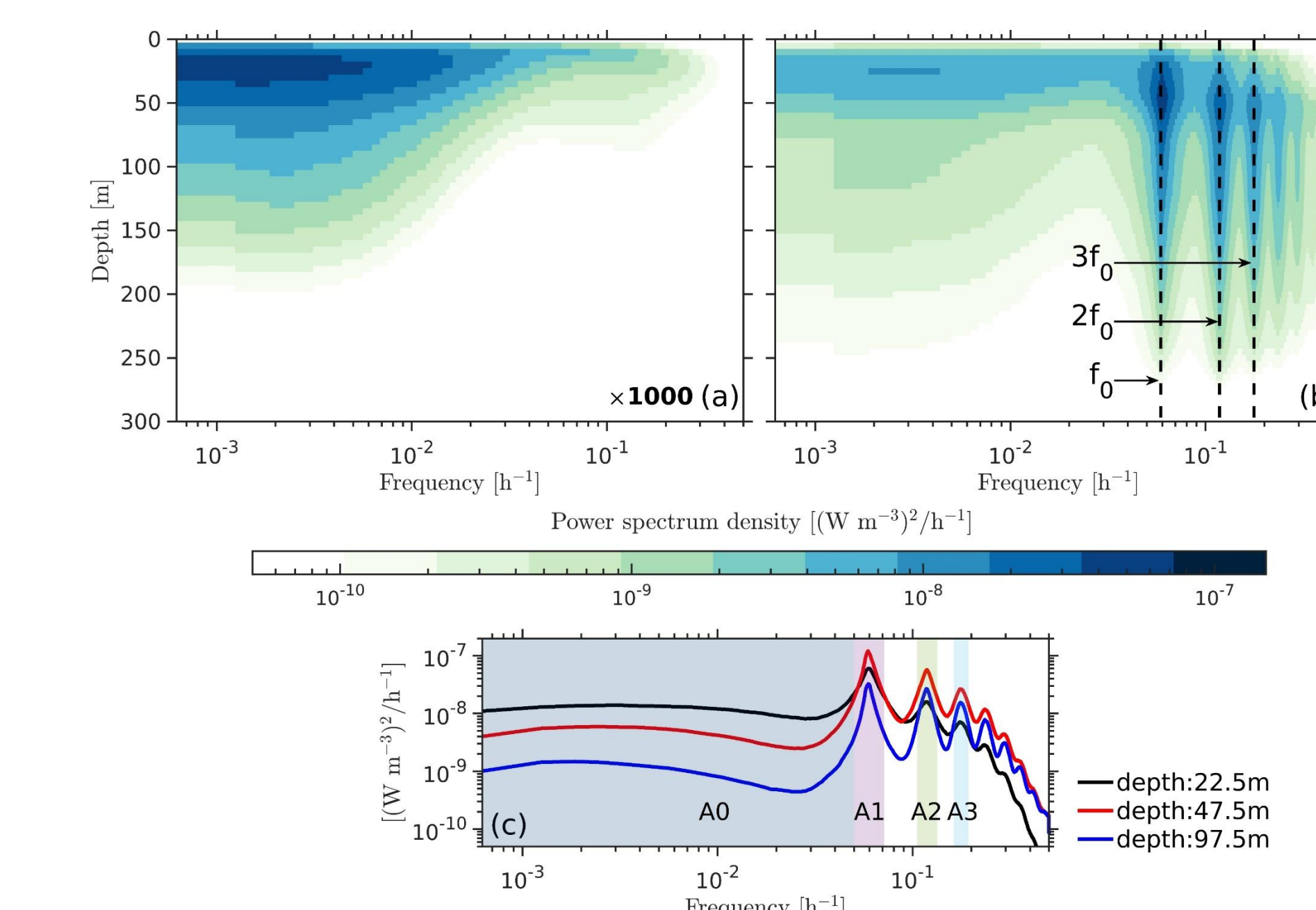


Figure 6 Frequency spectrum  $c(p_e, k_e)$ . (a) The unforced run. (b) The forced run. (c) The forced run at three depths.

- Converting activity between  $P_e$  and  $K_e$  is governed by inertial and superinertial motions.

## What We Got?

- In contrast to the result of the unforced run,  $K_e$  increased approximately nine times in the mixed layer and considerably in the pycnocline in the forced run.

- Eddies and filaments were seen to re-stratify the mixed layer and wind-induced turbulence at the base of the mixed layer promoted its deepening and therefore dramatically enhanced the exchange between  $K_e$  and eddy available potential energy  $P_e$ .

- The wind also excited inertial and superinertial motions throughout almost the whole water column.

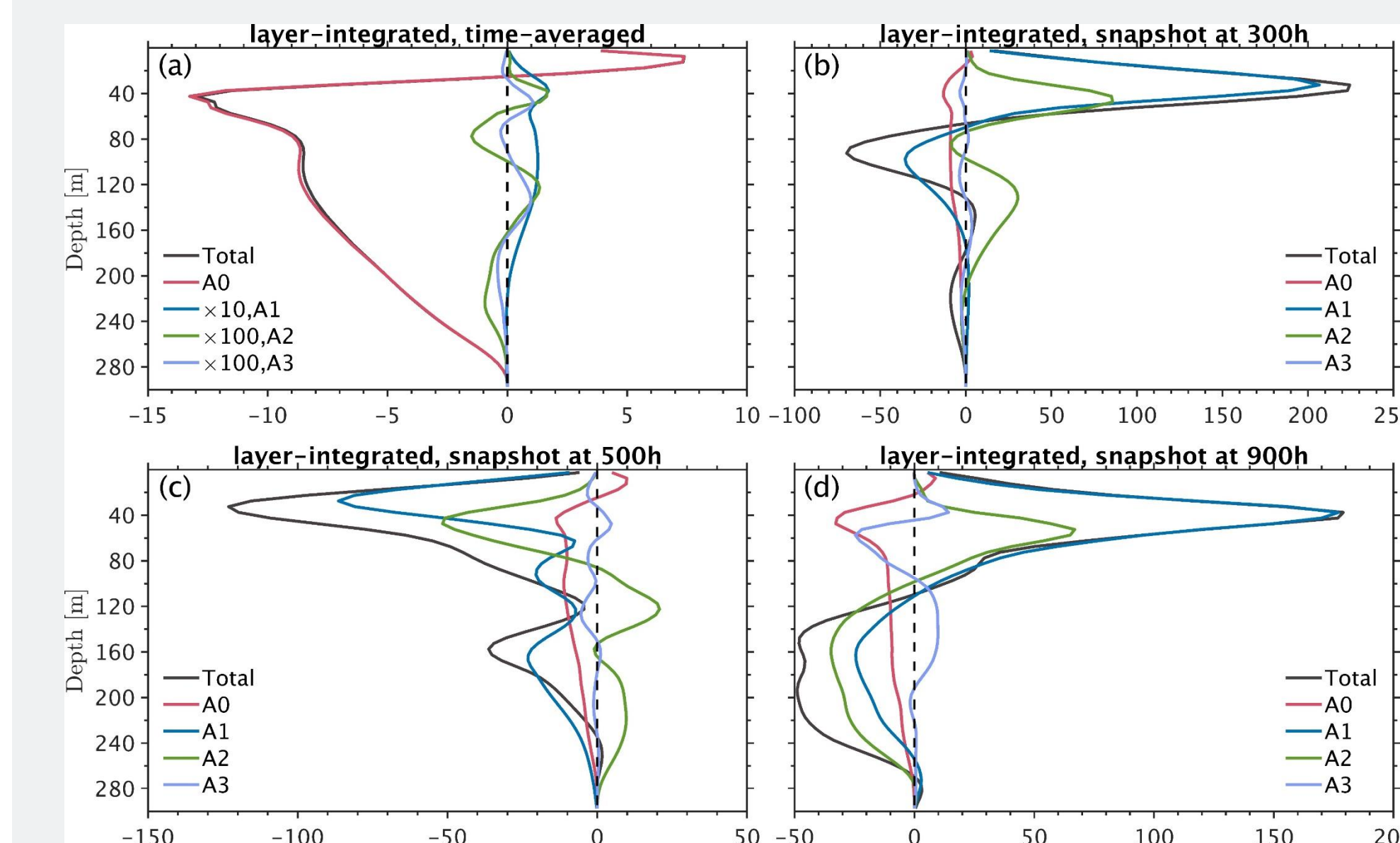


Figure 7 Layer-integrated  $c(p_e, k_e)$  for the time-averaged field and the snapshots at three time steps.

- Inertial and superinertial motions dominate the conversion process at each time but the gain effect over time is mainly contributed by the subinertial motions.

## Acknowledgement

Song Li acknowledges the financial support by China Scholarship Council (CSC). All numerical simulations were performed at the Deutsches Klimarechenzentrum (DKRZ), Hamburg, Germany.



©Authors. All rights reserved.

Center For Earth system Research AND Sustainability (CEN)

www.cen.uni-hamburg.de